Poly(Styrene Sulfonate) Self-Organization: Electrostatic and Secondary Interactions

H. Ahrens,[1] *K. Büscher,*[1,2] *D. Eck,*[2] *S. Förster,*[3] *C. Luap,*[4,5] *G. Papastavrou,*[1] *J. Schmitt,*[2] *R. Steitz,*[5,6] *C. A. Helm* *[1,2]

[1] Institut für Physik, Universität Greifswald, D-17489 Greifswald, Germany

[2] Institut für Physikalische Chemie, Universität Mainz, D-55099 Mainz, Germany

[3] Institut für Physikalische Chemie, Universität Hamburg, D-20146 Hamburg, Germany

[4] Stranski-Laboratorium, TU Berlin, Straße des 17. Juni 112, D-10623 Berlin, Germany

[5] BENSC, Hahn-Meitner Institut, Glienicker Straße 100, D-14109 Berlin, Germany

[6] MPI of Colloids and Interfaces, D-14424 Potsdam, P.O. Box 5607, Germany

Summary: We investigate the self-organization of PSS in brushes and polyelectrolyte multilayers with X-ray, neutron and optical reflectivity. The electrostatic force dominates brush phases and adsorption behavior, additionally we find evidence of a strong hydrophobic force: (ι) within amphiphilic diblock copolymer monolayers, a PSS monolayer adsorbs flatly to the hydrophobic block, (ιι) on temperature increase (and with screened electrostatic forces), more PSS is adsorbed onto oppositely charged surfaces, and (ιιι) a polyelectrolyte multilayers shrinks when heated at 100% r.h. The latter two effects are consistent with the well-known increase of the hydrophobic force on heating: The increased PSS surface coverage can be attributed to deteriorating solvent conditions. Within a polyelectrolyte multilayer, an increase of the hydrophobic force maximizes the local contact of hydrophobic polymer segments, causing a reduction of swelling and an increased mass density.

Keywords: monolayers; polyelectrolytes; self-organization

 DOI: 10.1002/masy.200450707

Introduction

Polyelectrolytes remain among the least understood materials in condensed matter science, despite their widespread presence and use. They are difficult to understand because of the entwined correlations of chain configuration and charge, coupled with the long-ranged interactions inherent to these structures. Yet, in the past decade the field of nanostructured material formation has progressed significantly. Self-assembly processes of polyelectrolytes involving electrostatic interactions can be used to build-up multilayered materials with unique properties. The basic principle is the sequential adsorption of positively and negatively charged polyelectrolytes.[1,2] Therefore, polyelectrolyte multilayers form two-dimensionally stratified layers which are growing step-by-step into the third dimension. This leads to a behaviour being dominated by internal interfaces and local interactions, and differing largely from the corresponding volume material properties.

Polyelectrolyte adsorption into an oppositely charged interface is determined by electrostatic and secondary interactions.[3,4] While the electrostatic interactions are qualitatively understood, little is known about the nature, the origin and the influence of the secondary forces.[5]

The flat conformation of polyelectrolytes adsorbed from salt solutions of low concentrations (i.e. below 0.1 Mol/L) is attributed to the large amplitude and range of the electrostatic force.[3] At high salt concentrations, both the polyelectrolyte coverage and the thickness of the adsorbed layer increase, features which are attributed to the screening of the electrostatic force.[6] Therefore, the respective strength of secondary forces such as segment/interface interaction and the polymer-solvent interaction (parameter w) start to be important. For w=0 (good solvent conditions) entropy dominates. For large w, polymer-solvent contact is unfavourable, the chain contracts, and, for very large w, the polymer precipitates. The transition is gradual, on increase of w, more polymer is adsorbed onto a surface.[7]

If the solvent is water, apolar or hydrophobic molecular groups of the polymer induce "bad solvent conditions".[8] An apolar molecule cannot form hydrogen bonds with water molecules, so it distorts the usual water structure, forcing the water into a rigid cage of hydrogen-bonded molecules around it. Water molecules as typical solvent molecules are normally in constant motion, and cage formation restricts the motion of a number of water molecules. This effect increases the structural organization of water, and thus decreases the entropy of the water molecules. If two hydrophobic groups aggregate, only one cage needs to be formed and fewer water molecules are confined. Therefore, hydrophobic groups are attracted towards each other,

forming so-called hydrophobic bonds. The hydrophobic interaction increases on heating, because of the increased water mobility. A prominent example are microtubules (one of the three cytoskeletal systems involved in cell motility and the determination of cell shape), which polymerize due to hydrophobic bonds. On temperature decrease to 4°C, they depolymerize. The microtubules repolymerize at 37°C (if a suitable protein as catalysator is present).

In this paper, we will focus on poly (styrene sulfonic acid) (PSS), a strongly charged polyelectrolyte with a hydrophobic backbone, which is no water-soluble if neutral.[9] It precipitates, if the temperature is increased to 60°C, an indication of strong secondary (possibly hydrophobic) interactions. We investigate the self-organization of PSS at interfaces, and explore different effects: polyelectrolyte brush phases,[10,11] polyelectrolyte multilayer build-up as function of composition and temperature of the adsorption solution,[12] polyelectrolyte multilayers and their swelling (because of the possible application as humidity sensor).[13]

Experimental Part

For polyelectrolyte multilayer preparation, PSS (M_w=84 kDa, M_w/M_n~1.1) served as polyanion, poly (allylamine) hydrocholoride (PAH, M_w=50-65 kDa) as polycation. To form an amphiphilic diblock copolymer monolayer, Poly(ethyl ethylene) (PEE) served as the hydrophobic block, PSS as the hydrophilic block (cf. Fig. 1).

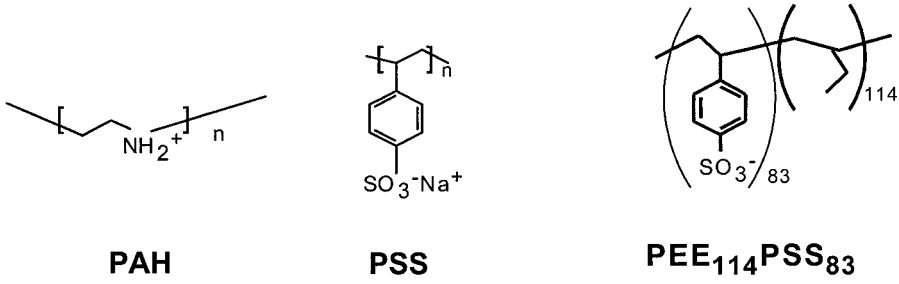

Figure 1. Scheme of PAH, PSS and of $PEE_{114}PSS_{83}$.

Specular X-ray reflectivity experiments on solid substrates were performed with a Siemens D-500 powder diffractometer. The X-ray set-up for fluid surfaces is home-built (λ=1.54Å),[14] its angular divergence is 0.012°. The neutron set-up is experiment V6 at HMI, (wavelength λ = 4.66 Å), in the liquid scattering set-up[15] and PNR reflectometer at GKSS Research Center for solid surfaces (wavelength λ = 6.37 Å). The relative humidity (r.h.) was adjusted with salt solutions.

For X-rays and neutrons, the specular reflection geometry is used, and the reflectivity is measured varying the angle of incidence α. The reflected intensity is measured as function of the wave vector transfer $Q_z = 4\pi \sin\alpha / \lambda$. The index of reflection n depends linearly on known material constants, and the electron density ρ or the scattering length density ρ_n, respectively: $n = 1 - r_o \rho \lambda^2 / 2\pi$ (Thompson radius $r_o = 2.82 \times 10^{-15}$ m) or $n = 1 - \rho_n \lambda^2 / 2\pi$. The reflectivity is calculated using classical Fresnel optics. To quantify the density profile, the exact matrix formalism is used.[16] In case of ambiguity, we chose the least structured profile (maximum entropy approach[17]), with which the measured reflectivity could be fitted.

Optical reflectivity experiments were performed in a UV-Vis spectrometer (Perkin-Elmer), using vertical incidence and varying wavelength. Now, the wave vector transfer corresponds to $Q_z = 4\pi / \lambda$. Depending on the environment the refractive index varies between 1.45 and 1.61. The same algorithms were used for analysis of the optical data as for X-ray and neutron reflectivity.

Atomic Force measurements (AFM) measurements were performed with a Multimode equipped with a Nanoscope IIIa (Digital Instruments; Santa Barbara, CA) in the tapping mode in air, and tips with 15 nm radius (according to the supplier, Olympus, Germany).

Results and Discussion

1. The inner interface of a PEE-PSS/water diblock copolymer monolayer

We investigated monolayers of $PEE_{114}PSS_{83}$ at the air/water interface, to characterize polyelectrolyte brushes.[10,11] Hydrophobic PEE is a suitable anchor for PSS, since it is fluid at room temperature, therefore, the PEE-PSS joints attain a new equilibrium distribution after a change in the grafting density.

To characterize the polyelectrolyte brushes, the electron density profiles of the monolayers are determined with X-ray reflectivity as function of the grafting density and the salt conditions. Extreme cases are shown in Fig. 2: pure water, or 1 M CsCl solution. X-ray reflectivity measurements are taken along the isotherm. The reflectivity curves show a very clear structure. At low Q_z, a thick layer (the PSS block) causes one narrow minimum, between two narrow maxima. On monolayer compression, the position is constant on pure water, whereas it shifts dramatically on the concentrated electrolyte solution. A thinner layer (the PEE block) causes the

minimum at high Q_z, which shifts on increase of the grafting density to lower Q_z, indicating thickening of the PEE block.

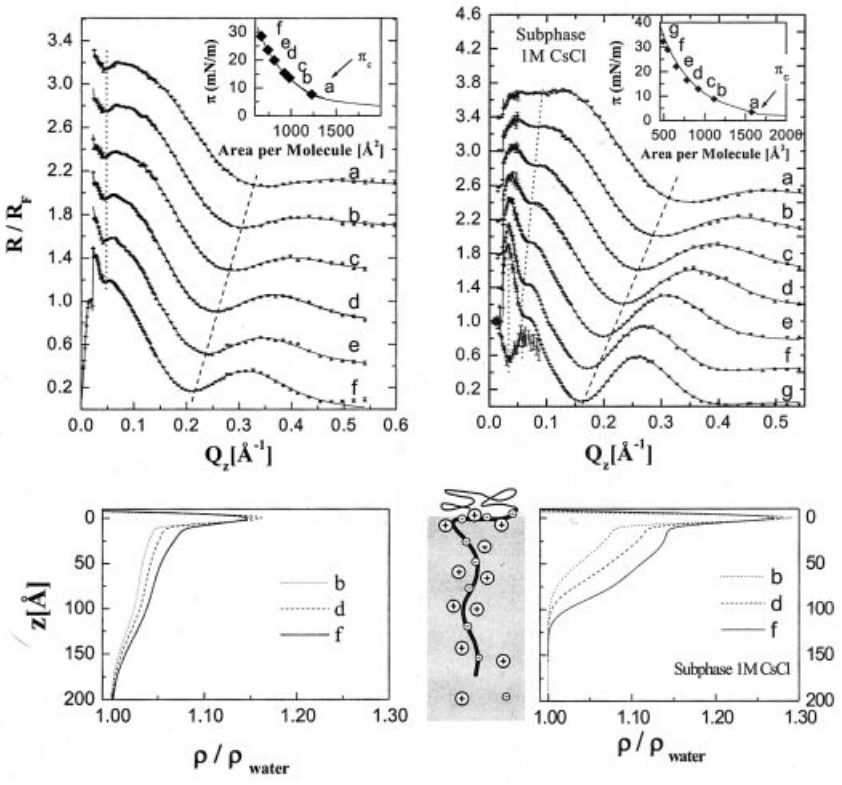

Figure 2. Normalized X-ray reflectivity from the diblock copolymer $PEE_{114}PSS_{83}$ on a subphase of pure water (top, left) or a 1M CsCl solution (top, right). The measurements were taken along the isotherm given in the inset, π_c indicates the formation of a homogeneous hydrophobic block. Below curve "g" a normalized neutron reflectivity curve taken at the same molecular area as "g" is shown. The full lines correspond to a fit of the electron (scattering length) density profiles to the data. The dashed lines are drawn through minima of equal order, as a guide to the eye. For clarity the reflectivity curves are shifted by 0.4 units. Bottom: electron density profiles of the PSS-brush at the molecular areas given in the inset. The 12Å thick layer of increased electron density is a PSS monolayer (including its counterions) which is flatly adsorbed to the PEE block.

The neutron reflectivity data show the same periodicity as found with X-rays at the same molecular area (1 Mol/l CsCl, D_2O instead of H_2O, cf. Fig. 2). The interference pattern is shifted by π, since for neutrons the subphase exhibits a higher scattering length density than the polyelectrolyte brush, while for X-rays the situation is inverted. Yet the interference pattern can be fitted with the same segment density profile as the X-ray data (considering that the PEE-layer is not accessible for neutron scattering, due to the limited Q_z-range). Since the counterions provide most of the contrast for X-rays, whereas for neutrons the contrast is due to the polymer segments only, this is direct evidence that the counterions do indeed trace the polymer closely.

As expected, the hydrophobic PEE block shows features characteristic of a melt: independence of the subphase, a constant electron density, and a linear increase of the thickness with the grafting density. Furthermore, two polyelectrolyte brush phases can be distinguished: at low salt the osmotically swollen brush characterized by stochiometric ion incorporation and almost constant thickness; at high salt (> 0.1 M) the salted brush, which shrinks both when the molecular area or subphase salt concentration is increased, according to power laws, as theoretically predicted[18]. Unexpectedly, directly beneath the hydrophobic anchors is a ~12Å thick layer of high electron density, which is attributed to a flat monolayer of PSS-chains.[10,11] When the PEE-layer is homogeneous (i.e. above π_c) the lateral density of this monolayer is constant (1 monomer per 44 $Å^2$) and independent of the grafting density, the PSS length, the polyelectrolyte brush phase, the concentration or the type of ions. Within this monolayer, one monomer is hydrated by 5-6 water molecules, and neutralized by one counterion (in Fig. 2, the measured electron density of the adsorbed PSS monolayer depends on the counterions in the subphase, either Cs^+ with its 54 electrons, or protons with no electrons). Only when the PEE-layer is no longer homogeneous (i.e. below π_c), the lateral density of the flatly adsorbed monolayer decreases. Obviously, there is strong attraction between PSS and PEE, which can be ascribed to hydrophobic interaction.

The importance of the hydrophobic force for PSS adsorption was confirmed by other studies, such as mixed monolayers of polyelectrolytes and surfactants at the air-water interface[19], or of PSS adsorbed directly to the water surface.[6,20]

2. Build-up of polyelectrolyte multilayers at different temperatures

The formation of polyelectrolyte multilayers is generally discussed as the consequence of multiple electrostatic bonds. Yet, other attractive interactions can also contribute. As described

above, PSS (as part of a diblock copolymer monolayer) adsorbs onto a hydrophobic surface, therefore it is likely that the hydrophobic force influences polyelectrolyte multilayer formation, too. This is studied by varying the deposition temperature under high salt conditions,[12] when both the amplitude and the range of electrostatic interactions are strongly screened,[3,21]

X-ray reflectivity curves from polyelectrolyte multilayers deposited at different temperatures are shown in Fig. 3. The thickness of the polyelectrolyte multilayer can be approximated from the average spacing Δq of the interference minima according to $d = 2\pi / \Delta q$. Two effects are obvious: on increase of build-up temperature, the interference minima shift continuously to the left, indicating film thickening. At 30°C and higher deposition temperatures, the amplitudes of the interference extrema decrease. The effect is especially obvious for higher order maxima, an effect which suggests roughening of the film/air interface. The polyelectrolyte multilayer thickness is increased by 40 % (1M KCl adsorption solution), or 20% (2M KCl), respectively.

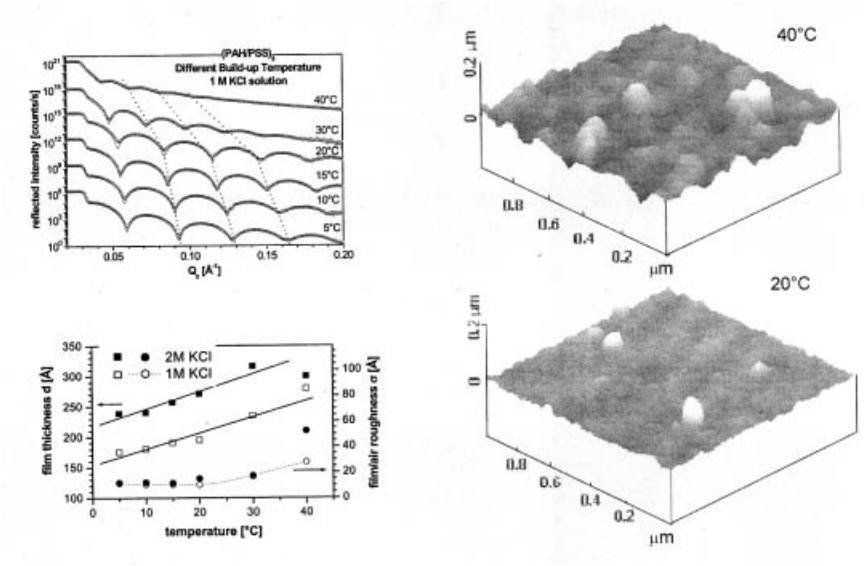

Figure 3. Top left: X-ray reflectivity curves of a 5 layer pair PSS/PAH-film, prepared from 1 M KCl solution at T=5, 10, 15, 20, 30, and 40°C, as indicated. For clarity, the X-ray reflectivity curves are shifted relative to each other, the dashed lines connecting the minima of equal order are guides to the eye. Bottom left: the film thickness (squares) and the roughness (circles) as function of the solution temperature, both for adsorption baths containing 1 M KCl (open symbols) and 2 M KCl (full symbols). Right: AFM images taken in the tapping mode of films prepared from 1 M KCl solution at 20 and 40°C, as indicated.

To explore the lateral extension of height fluctuations on the film surface, AFM images of the multilayers are shown in Fig. 3. The lateral extension of the height fluctuations, presumably polyelectrolyte aggregates, amounts to 50 – 200 nm. With the exception of the sample prepared from 2 M KCl solution at 40°C, the roughness $\sigma = \sqrt{\left(\sum_{i=1}^{N}\left(z_i - z_m\right)^2\right)/N}$ (z_m: average height, N: number of height measurements taken) is about a factor of two larger than the values obtained from X-ray reflectivity. Performing AFM measurements on surfaces covered with protruding polymer aggregates leads to "wrong" results with respect to the lateral aggregate dimensions, due to the convolution of the real aggregate size with the tip size.[22] Obviously, with polyelectrolyte multilayers, this convolution leads to an exaggerated roughness. The polyelectrolyte multilayers prepared at 40°C from 2 M KCl solution show a widely scattering roughness: x-ray reflectivity yields 52Å, AFM 12Å (the lowest value observed for the whole series). This scatter indicates pronounced lateral inhomogeneities, which is consistent with the severe stability problems during multilayer build-up at these conditions.

On heating a solution of macromolecules, water becomes a progressively bad solvent for hydrophobic groups[8]. For PSS we observe the analogous effect: on approaching the precipitation temperature, the polymer/solvent interaction increases. Therefore, more polyelectrolyte is adsorbed. A characteristic feature of surfaces covered with adsorbed neutral polymers is the dependence of the surface coverage on the polymer weight.[7] Yet, we do not find any molecular weight dependence,[12] indicating a still dominant role of the electrostatic forces.[3] Even though the increased layer thickness at elevated temperatures suggests an increasing importance of weak non-electrostatic bonds. Due to growing percentage of weak bonds, a polyelectrolyte molecule adsorbed at elevated temperature is more susceptible to desorption, lateral movement, etc. Indeed, we observe an increase in surface roughness.

3. Swelling of polyelectrolyte multilayers at different temperatures

To investigate the possible application of polyelectrolyte multilayers as humidity sensors, polyelectrolyte swelling was studied as function of relative humidity (r.h.), temperature and time. At 22°C, both the multilayer thickness and the water uptake (i.e. the scattering length density) increase linearly with the relative humidity, the thickness increase is about 29%,[13,23,24] corresponding to six water molecules per PAH/PSS monomer pair. With optical reflectivity,[13] the

kinetics of the swelling and shrinking are studied. On change of the r.h., equilibrium is attained within a second. Thus the film may be described as a mesh consisting of many voids, to which water molecules adsorb or from which they desorb. The flexible cavities change their size accordingly, and cause film swelling. If one furthermore considers the linear increase of both thickness and water content on r.h. change, it makes sense to describe the swelling at constant temperature in terms of a Langmuir isotherm. This approach yields a water binding energy of Q=33kJ/mol.

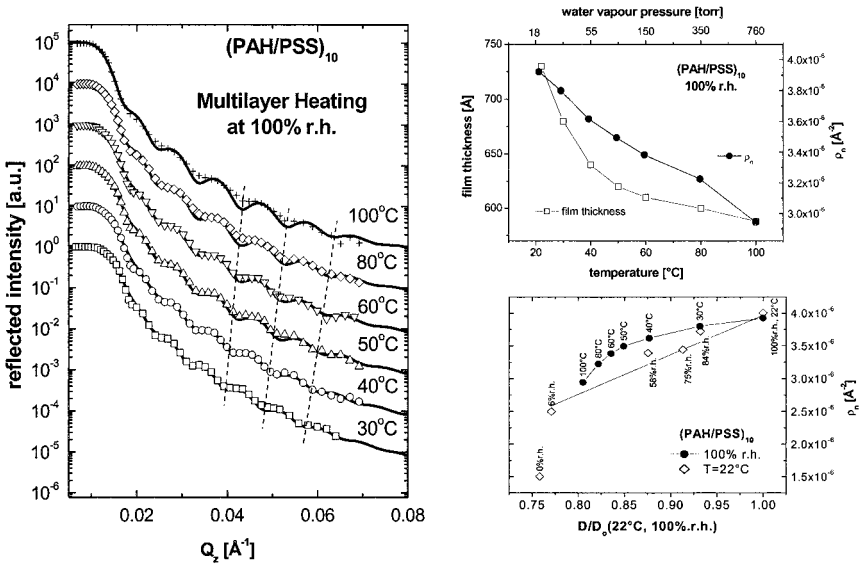

Figure 4. Left: Neutron reflectivity measurements of a 10 layer pair PSS/PAH-film (prepared at room temperature from 3 M NaCl solution) in a saturated D_2O-atmosphere at T=30, 40, 50, 80, and 100°C (bottom to top). Symbols represent data, solid lines the best fits. The reflectivity curves are shifted for the sake of clarity. The dashed lines are drawn through minima of equal order, as a guide to the eye. Top right: Film thickness (open squares) and scattering length density ρ_n (solid circles) as a function of temperature as derived from the fits shown left. Bottom right: Scattering length density as function of temperature. One film was investigated while increasing the temperature (solid circles, c.f. a,b) in a saturated D_2O atmosphere, the other one while varying the r.h. at T=22°C (open diamonds). Increasing the r.h. from 0 to 6% in a D_2O atmosphere causes a jump in the scattering length density (from 1.5×10^{-6}Å^{-2} to 2.5×10^{-6}Å^{-2}), due to the replacement of protons with deuterium in the ammonium groups (PAH->PAD). For the measurements at constant temperature, the solid line is a linear fit. The other line is a guide to the eye.

Doing heating experiments at 100% r.h., one has to realize that the water vapor pressure increases with the temperature according to $p_V = be^{-Q/RT}$ with b=76.8 GPa and Q=42.03 kJ/mol. Neutron reflectivity measurements of a $(PSS/PAH)_{10}$ film (prepared from 3 M NaCl solutions at room temperature) in a saturated D_2O-atmosphere at T=30, 40, 50, 60, 80, and 100°C are shown in Fig. 4(a).[13] The interference minima shift continuously to the right, indicating film thinning and water desorption. Careful data analysis reveals that the thickness decrease is accompanied by a slower than linear decrease of the scattering length density (cf. Fig. 4(b)), indicating not only water desorption, but also more efficient packing of some molecular groups.

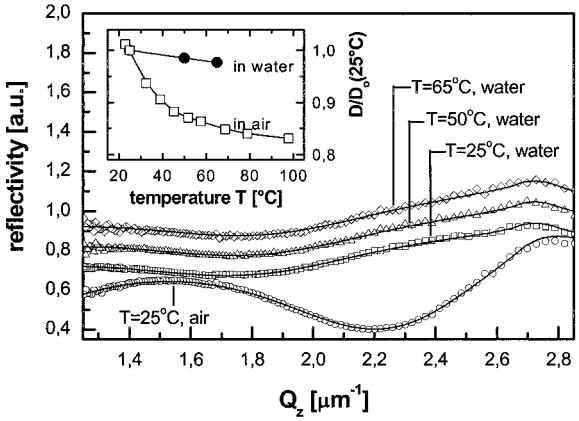

Figure 5. Optical reflectivity of a 32 layer pair PSS/PAH-film (prepared at room temperature from 3 M NaCl solution) on silicon. From bottom to top: in air, 25°C at ambient conditions, in H_2O at 25, 50 and 65°C. Symbols represent data points, solid lines corresponding fits. The reflection spectra are shifted for a better comparison. Inset: Normalized thickness ($D/D_o(25°C)$) vs. temperature for the 32 layer pair films in air (ambient conditions) and in water.

Even though the water vapor pressure increases due to heating, water molecules are expelled from the film, also its mass density increases. To explore the film shrinking at constant water chemical potential, the films were immersed in water, and their thickness is measured with optical reflectivity (cf. Fig. 5). On heating, again film shrinking is observed, yet it is substantially

less than at in humid air, only 3%. With optical reflectivity, the thickness changes on temperature increase were measured. They take hours. The long time scale indicates that polymer rearrangement occurs, a fact which is consistent with the increased mass density of the heated films at 100% r.h.

The film shrinking and the increased mass density can be attributed to a force, which increases both the attraction between polymer segments, and repels water from the monomers. This fact, together with the pronounced temperature dependence[13] confirms that within a PSS/PAH multilayer, local interactions of hydrophobic nature exist and influence the polymer conformation.

Conclusion and Outlook

We investigated the self-organization of PSS at interfaces, and explored different effects: We identified and characterized the theoretically predicted polyelectrolyte brush phases.[10,11] We studied polyelectrolyte multilayer build-up as function of concentration and kind of salt, as well as temperature, and confirmed the increased layer thickness with increasing salt concentration.[12] We were interested in polyelectrolyte multilayers as humidity sensors, and studied swelling.[13] In all cases, we found evidence of a strong hydrophobic force, which showed the characteristic temperature behavior.

In diblock copolymer monolayers at the air/water interface, besides the polyelectrolyte brush phases we always find a flatly adsorbed PSS monolayer beneath the hydrophobic block.[10,11] Obviously, PSS experiences a strong attraction by a hydrophobic surface.

When the temperature[8] during polyelectrolyte multilayer build-up is varied between 5 to 40°C (at high salt conditions, which reduce range and amplitude of the electrostatic force), a thickness increase of up to 40% is observed. Simultaneously, the film/air roughness increases. Both the larger thickness and the roughening are indicative of an increased percentage of weak non-electrostatic bonds within the film. The temperature dependence of these effects is consistent with the hydrophobic force.

Studying the swelling of polyelectrolyte multilayers, we unintentionally probed the local interactions. At room temperature, the thickness and the water content increase fast (equilibrium attained in less than 1 s) and linearly with the partial water pressure (i.e. the r.h.). Therefore, the film can be seen as a mesh consisting of many voids, to which water molecules adsorb or from which they desorb. However, on heating at 100% r.h., the behavior is very different: the film

shrinks while its mass density increases. It takes hours, until equilibrium is attained. Obviously, the polymer chains rearrange, increasing the packing efficiency. The hydrophobic segments are attracted to each other more strongly, and maximize their contact while the binding of water molecules is minimized.

We report very different experiments concerning the adsorption of PSS to hydrophobic and oppositely charged surfaces, as well as rearrangements within nanocomposits consisting partly of PSS. All observations are consistent with strong electrostatic forces. Yet for PSS, the hydrophobic force is obviously the most relevant of the secondary interactions, for other polyelectrolytes it may be different. There are other secondary interactions, like hydration forces, van der Waals interaction, specific forces, etc.[21] With the exception of some biological polymers and proteins, most polyelectrolytes have hydrophobic groups. To clarify the hierarchy of interactions during the self-assembly of polyelectrolytes much more experiments are necessary.

Acknowledgement

We thank Paul Simon and Karlheinz Graf for the help with the reflectivity experiments. The financial support of the DFG (He 1616/7-4) and the BMBF (03C0291C/5) are gratefully acknowledged.

[1]G. Decher, *Science* **277,** 1232-1237 (1997).

[2]M. Schönhoff, *Curr. Opin. Colloid Interface Sci.* **in print** (2003).

[3]R. R. Netz and J.-F. Joanny, *Macromolecules* **32,** 9013-9025 (1999).

[4]R. R. Netz, *J. of Phys. - Condensed Matter* **15,** s239-s244 (2003).

[5]S. S. Shiratori and M. F. Rubner, *Macromolecules* **33,** 4213-4219 (2000).

[6]H. Ahrens, H. Baltes, J. Schmitt, H. Möhwald, and C. A. Helm, *Macromolecules* **34,** 4504-4512 (2001).

[7]G. J. Fleer, M. A. C. Stuart, J. M. H. M. Scheutjens, T. Cosgrove, and B. Vincent, *Polymers at Interfaces* (Chapman and Hall, London, 1993).

[8]H. Lodish, A. Berk, S. L. Zipursky, P. Matsudaira, D. Baltimore, and J. Darnell, *Molecular Cell Biology*, 4th ed. (W.H. Freeman and Company, New York, 2000).

[9]S. Förster and M. Schmidt, *Advances in Polymer Science* **120,** 51-133 (1995).

[10]H. Ahrens, S. Förster, and C. A. Helm, *Macromolecules* **30,** 8447-8452 (1997).

[11]H. Ahrens, S. Förster, and C. A. Helm, *Phys. Rev. Lett.* **81,** 4172-4175 (1998).

[12]K. Büscher, H. Ahrens, K. Graf, and C. A. Helm, *Langmuir* **18,** 3885-3591 (2002).

[13]J. Schmitt, D. Eck, P. Simon, and C. A. Helm, **subm.** (2003).

[14]H. Baltes, M. Schwendler, C. A. Helm, and H. Möhwald, *J. Colloid and Interface Science* **178,** 135-143 (1996).

[15]R. Sedev, R. Steitz, and G. H. Findenegg, *Physica B* **315,** 267-272 (2002).

[16]L. G. Parratt, *Phys. Rev.* **95,** 359 (1954).

[17]J. S. Pedersen and I. W. Hamley, *J. Appl. Cryst.* **27,** 36-49 (1994).

[18]O. V. Borisov, E. B. Zhulina, and T. M. Birshtein, *Macromolecules* **27,** 4795 (1994).

[19]A. Asnacios, R. Klitzing, and D. Langevin, *Colloids Surf. A* **167,** 189-197 (2000).

[20]H. Yim, M. Kent, A. Matheson, R. Ivkov, S. Satija, J. Majewski, and G. S. Smith, *Macromolecules* **33,** 6126-6133 (2000).

[21]J. N. Israelachvili, *Intermolecular and Surface Forces*, 2nd ed. (Academic Press, London, 1991).

[22]J. Schmitt, P. Mächtle, D. Eck, H. Möhwald, and C. A. Helm, *Langmuir* **15,** 3256-3266 (1999).

[23]M. Lösche, J. Schmitt, G. Decher, W. G. Bouwman, and K. Kjaer, *Macromolecules* **31,** 8893-8906 (1998).

[24]R. Kügler, J. Schmitt, and W. Knoll, *Macrom. Chem. Phys.* **203,** 413-419 (2002).